

Anticancer, antioxidant, DFT calculations, and docking studies of some new peptide-indole conjugates

Hasan Küçükbay ^{1*}, Zeynep Gönül ¹, Ali Kuruçay ¹, Burhan Ateş ¹, Housseem Boulebd ² and F. Zehra Küçükbay ³

¹Department of Chemistry, Faculty of Arts and Sciences, İnönü University, 44280 Malatya, Türkiye

² Department of Chemistry, Faculty of Exact Science, University of Constantine 1, Constantine, Algeria

³ Department of Basic Pharmaceutical Sciences, Faculty of Pharmacy, İnönü University, 44280 Malatya, Türkiye

(Received January 29, 2024; Revised March 20, 2024; Accepted March 21, 2024)

Abstract: In this study, the structures of six new peptide-indole derivatives were elucidated through spectroscopic and analytical methods following their synthesis. In addition to their anticancer and antioxidant properties, density functional theory (DFT) calculations and docking studies were conducted for the compounds. According to the obtained results, compounds **1** and **3** were identified as the most active against the MCF-7 cell line, with IC₅₀ values of 8.72 and 5.86 µg/mL, respectively. Conversely, compounds **4** and **1** were found to be the most active against the A549 cell line, with IC₅₀ values of 15.43 and 16.10 µg/mL, respectively. When compared to standard antioxidants using both the DPPH and iron reduction power assays, the compounds did not exhibit significant antioxidant activity. The molecular geometry and electronic properties of the synthesized peptide-indole derivatives were investigated through theoretical calculations using the Density Functional Theory (DFT) method. Molecular docking studies were also conducted to investigate the binding modes of the synthesized compounds within the active sites of EGFR enzyme.

Keywords: Indole derivatives; peptides; anticancer; antioxidant; DFT calculations; docking study. ©2024 ACG Publications. All right reserved

1. Introduction

The synthesis of nitrogen-containing heterocyclic compounds has always been a fascinating area of research in organic chemistry due to their diverse biological activities.^{1,2} Indole derivatives, a class of nitrogen-containing heterocyclic compounds, possess a wide range of physiological properties, and have therefore been integrated into the structure of many drugs.

The indole skeleton is a key component of numerous naturally occurring compounds, with important physiological³ and industrial properties⁴⁻⁷ Hence, indoles have become a crucial research topic in various fields such as pharmaceuticals, fragrances, agricultural control, pigments, and materials science^{8,9} One of the most significant indole derivatives is tryptophan, an essential amino acid and one

* Corresponding author: E-Mail: hasan.kucukbay@inonu.edu.tr; Phone: +90 5425871648

of the 22 naturally occurring amino acids. Although organisms cannot synthesize tryptophan, it can be obtained through daily nutrition. The essential amino acid tryptophan plays a crucial role in protein synthesis as a building block, and as a precursor in various vital biochemical processes carried out by functional proteins. Tryptophan analogs are also significant building blocks for natural product synthesis, peptidomimetics, and biologically active compounds.¹⁰

The indole structure is also found in indole-3-carbinol, which is an important antitumor agent¹¹. Controlled studies employing laboratory animals and cultured cells on indole-3-carbinol demonstrate its inhibition of aflatoxin binding. Consequently, the carcinogenic effects of aflatoxins are reduced.^{12,13} Tryptamine, as an additional notable derivative of indole, demonstrates a diverse range of bioactivity.¹⁴ In a recent study conducted in our research laboratory, we aimed to synthesize dipeptide derivatives of indole with known physiological activities. This was in response to the promising anticancer activities exhibited by 5-aminomethylindole-dipeptide derivatives against A2780 and MCF.¹⁵

In light of our noteworthy investigation into indole-related compounds, we have effectively synthesized six novel indole-dipeptide derivatives. The structural elucidation of these derivatives was accomplished, followed by an exploration of their potential as anticancer agents against A549 and A2740 cancer cell lines.

Theoretical calculations employing the Density Functional Theory (DFT) method via the Gaussian 09 software program were employed to analyze the molecular geometry and electronic characteristics of the peptide-indole derivatives that were synthesized. Additionally, molecular docking studies were carried out to explore the binding mechanisms of the newly synthesized peptide-indole conjugates within the active sites of the EGFR enzyme.

2. Experimental

2.1. Chemical Material and Apparatus

Standard techniques were employed to purify and dry all solvents before use. Commercially available reagents from Aldrich, Acros, ABCR, and Merck were used without further purification. Reactions involving compounds sensitive to air or moisture were conducted in dried glassware under an argon atmosphere. Analytical thin-layer chromatography (TLC) was performed on Sigma-Aldrich silica gel 60 F-254 aluminum plates. The human breast (MCF-7) cancer cell lines and human ovarian (A-2780) cancer cell lines were obtained from the American Type Culture Collection (ATCC). Nuclear magnetic resonance (¹H NMR, ¹³C NMR) spectra were recorded in DMSO-d₆ using a Bruker Advance III 400 MHz spectrometer. Chemical shifts were reported in parts per million (ppm) and the coupling constants (*J*) were expressed in Hertz (Hz). Exchangeable protons (NH) were confirmed by the addition of D₂O. Mass spectra were recorded on an Agilent Technologies 6530 Accurate-Mass Q-TOF-LC/MS. Elemental analyses were performed using the LECO CHNS-932 elemental analyzer. Infrared spectra were recorded in the range of 4000-650 cm⁻¹ using ATR equipment on a Perkin Elmer Spectrum one FTIR spectrophotometer. Melting points (m.p.) were measured in open capillary tubes using a Gallenkamp MPD350.BM3.5 apparatus and are reported without correction. All microwave-assisted reactions were carried out using a microwave oven system manufactured by Milestone (Milestone Start S Microwave Labstation for Synthesis).

Starting N-protected mono (**I**) and dipeptides (**II** and **III**) were prepared according to previously published procedures.¹⁵⁻¹⁸

2.2. Chemistry

2.2.1. General Synthesis Method of Peptide-Indole Conjugates (**1-5**)

To synthesize compounds **1-5**, compound **I** or **III** (1 mmol) was reacted with commercially available 1-methyl-3-aminomethylindole (1.2 mmol) in the presence of anhydrous THF (5.0 mL) at 70°C under microwave irradiation for one hour. The reaction progress was monitored by thin-layer chromatography. Afterward, all volatiles were removed by rotavapor, and the resulting crude product was crystallized from methanol, yielding compounds **1-5** at 64-89% yield.

New peptide-indole conjugates and their biological activities

Benzyl [(2R,3R)-3-methyl-1-[[[(1-methyl-1H-indol-3-yl)methyl]amino]-1-oxopentan-2-yl]carbamate (1): Cream solid (yield 84%); m.p: 194-195 °C; ¹H NMR (400 MHz, DMSO-*d*₆) δ (ppm): δ 8.18 (t, 1H, CH₂NH, *J* = 4.0 Hz), 7.57 (d, 1H, CHNH, *J* = 8.0 Hz), 7.41-7.14 (m, 8H, ArH), 7.01 (t, ArH, 1H, *J* = 8.0 Hz), 5.02 (s, 2H, CH₂O), 4.46-4.36 (m, 2H, NHCH₂-indole), 3.90 (t, 1H, NHCH, *J* = 8.0 Hz), 3.74 (s, 3H, CH₃), 1.73-1.68 (m, 1H, CHCHNH), 1.45-1.49 and 1.12-1.04 (dm, 2H, CHCH₂CH₃), 0.79-0.76 (m, 6H, CH₃CH₂ and CH₃CH); ¹³C NMR (101 MHz, DMSO-*d*₆) δ 171.4(CO), 156.5 (OCONO), 137.6, 137.2, 128.8, 128.6, 128.2, 128.1, 127.2, 121.7, 119.4, 119.0, 111.6, 110.0 (Ar-C), 65.8 (PhCH₂O), 59.7 (HNCH₂-indole), 36.9 (NCCHCH) 34.2 (NCH₃), 32.6 (CHCHNH), 24.8 (CHCH₂CH₃), 15.9 (CHCH₃), 11.4 (CH₂CH₃); IR (cm⁻¹): ν_{(C=O)ketone}: 1688 cm⁻¹, ν_{(C=O)carbamate}: 1639 cm⁻¹, ν_{(N-H)amine}: 3272 cm⁻¹; HRMS (Q-TOF): *m/z* [M+Na]⁺ calcd for C₂₄H₂₉N₃NaO₃: 430.2107, found: 430.2104; Elemental analysis: C₂₄H₂₉N₃O₃ required C, 70.74; H, 7.17; N, 10.31; found C, 70.72; H, 7.17; N, 10.36.

tert-Butyl (R)-1-[[[(1-methyl-1H-indol-3-yl)methyl]amino]-1-oxo-3-phenylpropan-2-yl]carbamate (2): Cream solid (yield 89%); m.p: 137-138 °C; ¹H NMR (400 MHz, DMSO-*d*₆) δ (ppm): δ 8.20 (t, 1H, NH, *J* = 5.3 Hz), 7.56 (d, 1H, NH, *J* = 7.9 Hz), 7.41 (d, 1H, ArH, *J* = 8.2 Hz), 7.27-7.13 (m, 7H, ArH), 7.10-6.85 (m, 2H, ArH), 4.55-4.31 (m, 2H, NHCH₂-indole), 4.20-4.14 (m, 1H, CHCH₂Ph), 3.75 (s, 3H, NCH₃), 2.92 (dd, 1H, CH₂Ph, *J* = 13.6, 4.5 Hz), 2.74 (dd, 1H, CH₂Ph, *J* = 13.5, 10.3 Hz), 1.30 (s, 9H, Me₃C); ¹³C NMR (101 MHz, DMSO-*d*₆) δ 171.8 (CO), 155.7 (OCONO), 138.7, 137.2, 129.8, 129.7, 128.4, 127.2, 126.6, 121.7, 119.44, 119.0, 111.9, 110.1 (Ar-C), 78.4 (Me₃CO), 56.3 (HNCH₂-indole), 38.2 (NHCHCH₂), 34.4 (NHCH₃), 32.8 (CH₂Ph), 28.6 [(CH₃)₃C]; IR (cm⁻¹): ν_{(C=O)ketone}: 1693 cm⁻¹, ν_{(C=O)carbamate}: 1629 cm⁻¹, ν_{(N-H)amine}: 3283 cm⁻¹; HRMS (Q-TOF): *m/z* [M+Na]⁺ calcd for C₂₄H₂₉N₃NaO₃: 430.2107, found: 430.2134; Elemental analysis: C₂₄H₂₉N₃O₃ required C, 70.74; H, 7.17; N, 10.31; found C, 70.73; H, 7.16; N, 10.33.

Benzyl (S)-1-[(2-[[[(1-methyl-1H-indol-3-yl)methyl]amino]-2-oxoethyl]amino]-4-(methylthio)-1-oxobutan-2-yl]carbamate(3): Cream solid (yield 76%); m.p: 126-127 °C; ¹H NMR (400 MHz, DMSO-*d*₆) δ (ppm): δ 8.26 (t, 1H, NH, *J* = 6.0 Hz), 8.07 (t, 1H, NH, *J* = 4.0 Hz), 7.54 (t, 1H, NH, *J* = 4.0 Hz), 7.38-7.31 (m, 7H, ArH), 7.23 (s, 1H, ArH), 5.03 (d, 2H, CH₂O, *J* = 4.0 Hz), 4.42-4.40 (m, 2H, NHCH₂-indole), 4.12-4.08 (m and bs, 3H, CH₂CO + CHNH), 3.78 (s, 3H, NCH₃), 2.49-2.44 (m, 2H, CH₂CH), 2.03 (s, 3H, SCH₃), 1.85-1.75 (m, 2H, CH₂SCH₃); ¹³C NMR (101 MHz, DMSO-*d*₆) δ 172.3 and 168.7 (CO), 156.6 (OCONO), 139.6, 137.2, 129.8, 128.8, 128.2, 128.1, 125.4, 122.0, 119.4, 115.5, 111.9, 110.3 (Ar-C), 66.6 (CH₂O), 54.5 (HNCH₂-indole), 34.6 (CH₂CO), 34.2 (NHCH), 32.9 (CH₃N), 32.7 (CH₂CH), 30.1 (SCH₃), 15.0 (CH₂SCH₃); IR (cm⁻¹): ν_{(C=O)ketone}: 1703 and 1664 cm⁻¹, ν_{(C=O)carbamate}: 1640 cm⁻¹, ν_{(N-H)amine}: 3280 cm⁻¹; HRMS (Q-TOF): *m/z* [M+Na]⁺ calcd for C₂₅H₃₀N₄NaO₄S: 505.1885, found: 505.1866; Elemental analysis: C₂₅H₃₀N₄O₄S required C, 62.22; H, 6.27; N, 11.61; found C, 62.19; H, 6.26; N, 11.65.

Benzyl [(S)-1-[(R)-1-[[[(1-methyl-1H-indol-3-yl)methyl]amino]-1-oxo-3-phenylpropan-2-yl]amino]-4-(methylthio)-1-oxobutan-2-yl]carbamate(4): Cream solid (yield 84%); m.p: 216-217 °C; ¹H NMR (400 MHz, DMSO-*d*₆) δ (ppm): δ 8.28 (t, 1H, NH, *J* = 6.0 Hz), 8.02 (d, 1H, NH, *J* = 8.0 Hz), 7.53 (t, 2H, ArH), 7.46-7.26 (m, 6H, ArH + NH), 7.26-7.13 (m, 7H, ArH), 7.03 (t, 1H, ArH, *J* = 8.0 Hz), 4.99 (q, 2H, CH₂O, *J* = 12.6 Hz), 4.54-4.53 (m, 1H, CHNH), 4.41 (d, 2H, NHCH₂-indole, *J* = 4.0 Hz), 4.07-4.05 (m, 1H, CHNH), 3.73 (s, 3H, NCH₃), 3.01-2.96 (m, 1H, CH₂Ph), 2.86-2.80 (m, 1H, CH₂Ph), 2.37-2.35 (m, 2H, CH₂CH₂S), 1.99 (s, 3H, SCH₃), 1.76-1.70 (m, 2H, CH₂SCH₃); ¹³C NMR (101 MHz, DMSO-*d*₆) δ 171.5 and 170.8 (CO), 156.4 (OCONO), 138.1, 137.4, 137.2, 129.7, 128.8, 128.4, 128.4, 128.3, 128.2, 127.2, 126.7, 121.7, 119.4, 119.1, 111.7, 110.1 (Ar-C), 66.0 (CH₂O), 54.6 (NHCH), 54.3 (HNCH₂-indole), 38.3 (NHCH), 43.4 (NCH₃), 34.4 (CH₂Ph), 32.7 (CH₂CH₂S), 30.0 (SCH₃), 15.0 (CH₂SCH₃); IR (cm⁻¹): ν_{(C=O)ketone}: 1700 and 1688 cm⁻¹, ν_{(C=O)carbamate}: 1630 cm⁻¹, ν_{(N-H)amine}: 3278 cm⁻¹; HRMS (Q-TOF): *m/z* [M+Na]⁺ calcd for C₃₂H₃₆N₄NaO₄S: 595.2355, found: 595.2342; Elemental analysis: C₃₂H₃₆N₄O₄S required C, 67.11; H, 6.34; N, 9.78; found C, 67.09; H, 6.34; N, 9.57.

tert-Butyl [(R)-1-[(S)-1-[[[(1-methyl-1H-indol-3-yl)methyl]amino]-1-oxo-3-phenylpropan-2-yl]amino]-1-oxo-3-phenylpropan-2-yl]carbamate (5): Cream solid (yield 78%); m.p: 145-146 °C; ¹H NMR (400 MHz, DMSO) δ 8.32 (bs, 1H, NH), 8.03 (d, 1H, NH, *J* = 7.8 Hz), 7.55 – 6.94 (m, 16H, ArH + NH), 4.59-4.54 (m, 1H, CHNH), 4.41 (bs, 2H, NHCH₂-indole), 4.15-4.09 (m, 1H, CHNH), 3.74 (s, 3H, NCH₃), 3.00 – 2.96 (m, 1H, CH₂Ph), 2.88-2.83 (m, 2H, CH₂Ph), 2.68-2.62 (m, 1H, CH₂Ph), 1.30 (s, 9H,

Me_3C); ^{13}C NMR (101 MHz, DMSO) δ 171.7(CO), , 170.8(CO), 155.6 (OCONO), 138.6, 138.0, 137.2, 129.8, 129.6, 128.4, 127.2, 126.7, 126.6, 125.5, 121.7, 119.4, 119.1, 115.4, 111.7, 110.1 (Ar-C), 78.6 (Me_3CO), 56.4 (NHCH), 54.2(HNCH₂-indole), 38.6 (NHCH), 38.0 (NCH₃), 34.4 (CH₂Ph), 32.8 (CH₂Ph), 28.6 [(CH₃)₃C]; IR (cm⁻¹): $\nu_{(C=O)ketone}$: 1722 and 1690 cm⁻¹, $\nu_{(C=O)carbamate}$: 1630 cm⁻¹, $\nu_{(N-H)amine}$: 3269 cm⁻¹; HRMS (Q-TOF): m/z [M+H]⁺ calcd for C₃₃H₃₉N₄O₄: 555.2971, found: 556.3042; Elemental analysis: C₃₂H₃₈N₄O₄ required C, 71.46; H, 6.91; N, 10.10; found C, 71.42; H, 6.91; N, 10.13.

(*S*)-1-(((*R*)-1-(((1-methyl-1*H*-indol-3-yl)methyl)amino)-1-oxo-3-phenylpropan-2-yl)amino)-1-oxo-3-phenylpropan-2-aminium 2,2,2-trifluoroacetate(**6**): Burgundy solid (yield 58%); m.p: 234-235 °C; 1H NMR (400 MHz, DMSO) δ 8.83 (bs, 3H, N⁺H₃), 8.18 (4, 1H, NH, *J* = 8.0 Hz), 7.56 – 7.16 (m, 15H, ArH + NH), 4.54–4.49 (m, 2H, NHCH₂-Indole), 4.39-4.36 (m, 1H, CHCH₂Ph), 4.27 4.19 (m, 1H, CHCH₂Ph), 4.05 (s, 3H, CH₃), 3.12-2.81 (m, 4H, CHCH₂Ph). ^{13}C NMR (101 MHz, DMSO) δ 172.7 (CO), 168.3 (CO), 158.4 (q, CF₃CO, $^2J_{(C-F)}$ = 30.0 Hz), 138.0, 136.4, 135.3, 133.7, 133.0, 130.6, 130.1, 129.7, 129.6, 128.9, 128.8, 128.7, 128.6, 127.6, 127.5, 126.9 (ArC), 117.6 (q, CF₃CO, $^1J_{(C-F)}$ = 300 Hz), 56.7 (HNCH₂-indole), 53.6 (CHCH₂Ph), 38.2(CHCH₂Ph), 37.4 (CH₂Ph), 30.2 (CH₂Ph), 29.9 [(CH₃)₃C]; IR (cm⁻¹): $\nu_{(C=O)ketone}$: 1669 cm⁻¹; HRMS (Q-TOF): m/z [M-F₃CCOO-]⁺ calcd for C₂₈H₃₃N₄O₂: 455.2442, found: 455.2000; Elemental analysis: C₃₀H₃₁F₃N₄O₄ required C, 63.37; H, 5.50; N, 9.85; found C, 63.34; H, 5.49; N, 9.91.

2.3. Biological Assay

2.3.1. Cytotoxicity Assay

MTT assay antitumor activities of these substances were evaluated by 3-(4,5dimethylthiazol-2-yl)-2,5-diphenyltetrazolium bromide (MTT) assay.¹⁹ MCF-7 (Human Breast Cancer) and A549 (Human Lung Cancer) cells were grown in a separate flask, in a 5% CO₂ incubator at 37 degrees, using high glucose DMEM medium, which is a mixture of 10% FBS and 1% Pen-Strep. 10000 MCF-7 cells in each well and 10000 A549 cells in another 96-well plate were seeded into 96-well plates. Each well plate was named and numbered, then allowed to adhere and spread in the CO₂ incubator until the next day. A solution of each dipeptide-indole derivative was first prepared with DMSO at 1 mg/mL and then diluted with medium to 6.25, 12.5, 25, 50, 100 and 200 μ g/mL concentrations. The waiting medium in the well plate was withdrawn and replaced with 100 μ L of the medium containing different dipeptide-indole conjugates and different concentrations. It was then incubated at 37 degrees for 24 hours in a 5% CO₂ incubator until the next day. MTT dye at 5 mg/mL was dissolved in PBS (pH: 7.4 in Phosphate Buffer). After 24 hours, the old medium from all well plates is discarded and replaced with 90 μ L of DMEM in each well and 10 μ L of 5mg/mL prepared MTT (3-(4,5-dimethylthiazol-2-yl)-2,5-diphenyltetrazolium bromide) in each well. 100 μ L of the mixture was prepared and incubated in a CO₂ incubator for 4 hours. After incubation, the medium with MTT in the well plates was withdrawn and discarded. 100 μ L of DMSO was added to each well of the well plates. The well plates were read with the help of a spectrophotometer device at 540 nm wavelengths immediately after DMSO was loaded.

2.3.2. Antioxidant Activity Assays

2.3.2.1. Radical Scavenging Activity Using DPPH Method

The radical scavenging activity of dipeptide-indole conjugates was assessed by their ability to act as antioxidants against the stable free radical, 1,1-diphenyl-2-picrylhydrazil (DPPH). The method suggested by Yang *et al.*,²⁰ was followed, wherein 1 mL of the antioxidant solution (dissolved in ethanol) was added to 3 mL of 0.1 mM ethanolic DPPH solution. The solutions were kept in the dark for 30 minutes at ambient temperature, and their absorbance readings were measured at 517 nm. The inhibition (%) was calculated using the following formula;

$$[1 - (As-Ao)/Ab] \times 100,$$

where As is the absorbance reading for samples including the antioxidant, Ao is the absorbance of the antioxidant in pure ethanol, and Ab corresponds to the absorbance of the DPPH solution. Positive

New peptide-indole conjugates and their biological activities

controls such as butylated hydroxyanisole (BHA), butylated hydroxytoluene (BHT), and α -tocopherol were employed in the study.

2.3.2.2. Ferric Ions Reducing Power Assay

The assessment of the reducing power of dipeptide-indole conjugates and standards adhered to the protocol outlined by Oyaizu.²¹ In summary, varying concentrations of the compounds (12.5, 25.0, and 37.5 $\mu\text{g/mL}$), dissolved in 1 mL ethanol, were combined with 2.5 mL of 0.2 M phosphate buffer (pH 6.6) and 2.5 mL of 1% potassium ferricyanide, followed by incubation at 50°C for 20 minutes. Subsequently, 2.5 mL of 10% trichloroacetic acid solution was introduced, and the resulting mixture underwent centrifugation at 3000 rpm for 10 minutes. The supernatant was amalgamated with 2.5 mL distilled water and 0.5 mL of 0.1% ferric chloride, and the absorbance was gauged at 700 nm against a blank consisting of distilled water and phosphate buffer. The reducing power assays were conducted in triplicate, with the elevation in absorbance within the reaction mixture serving as an indicator of the reducing power of the samples/standards. Positive controls, such as α -tocopherol, BHT, or BHA, were incorporated for reference.

2.4. Structural Features and Electronic Properties

2.4.1. DFT Calculations

The molecular geometry and electronic properties of the synthesized dipeptide-indole derivatives were investigated through theoretical calculations using the Density Functional Theory (DFT) method. The Gaussian 09 software was employed for all computations, utilizing the B3LYP functional in combination with the 6-311+G(d,p) basis set.²² confirm the ground states, the absence of imaginary frequencies was checked.

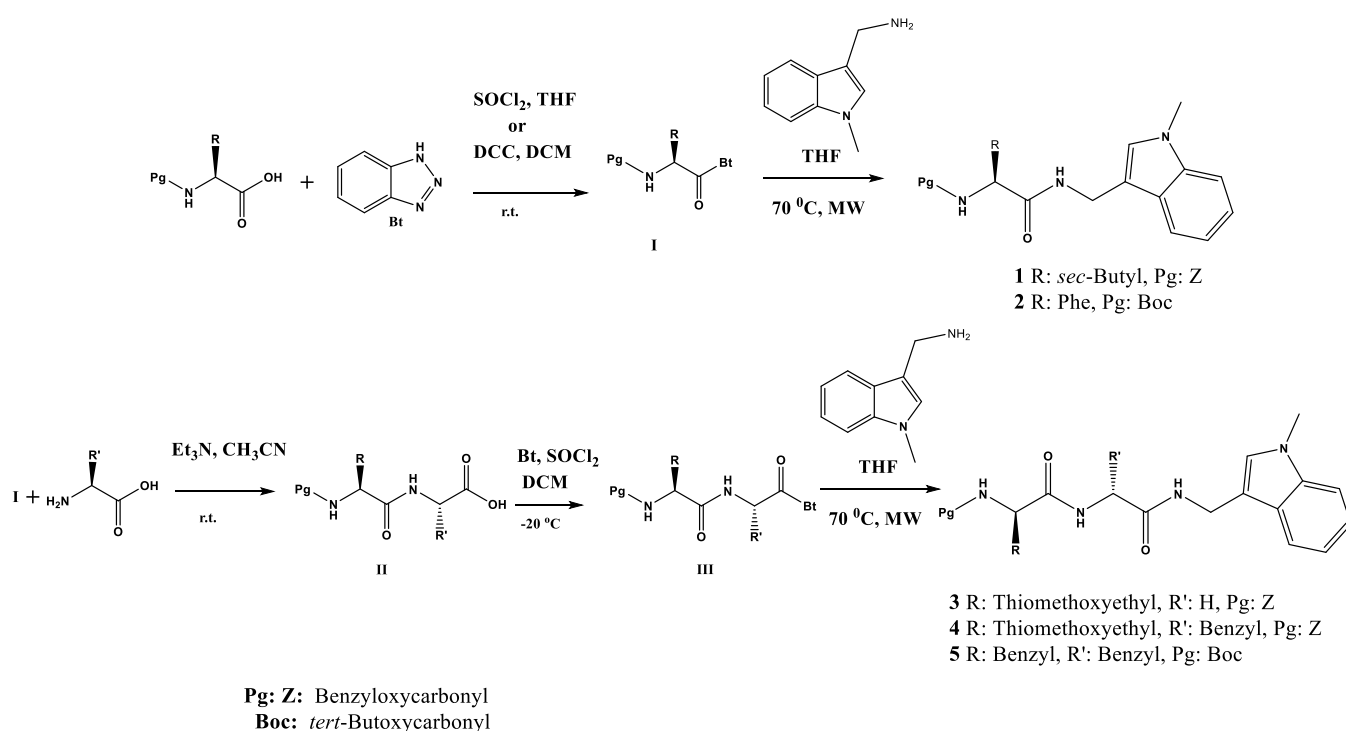
2.4.2. Molecular Docking

Molecular docking studies were conducted to investigate the binding modes of the synthesized compounds within the active sites of EGFR enzyme. The molecular geometries of the compounds were determined through DFT calculations. The coordinates of EGFR were retrieved from the Protein Data Bank (PDB) with the 2ITY identifier. The prepared protein structure involved the meticulous removal of ligands, water molecules, heteroatoms, and co-crystallized solvents. Subsequently, AutoDockTools (version 1.5.6) was employed to introduce partial charges and hydrogen atoms into both the protein and ligands. The search space for docking simulations was defined as a 25 Å cube with grid points spaced 1 Å apart, centered at the enzyme's active site. Docking studies were performed using AutoDock Vina (version 1.1.2),²³ with most default settings retained, except for 'num_modes,' which was set to 32 to ensure a thorough exploration of binding modes. For visualization and analysis of the results, BIOVIA Discovery Studio (available at <https://3dsbiovia.com/>) was utilized. The reliability and accuracy of the docking procedure were confirmed by comparing crystallographic data with theoretical data for native ligands, resulting in a root mean square deviation (RMSD) of less than 1.5 Å.

3. Results and Discussion

3.1. Chemistry

The mono- and dipeptide-indole derivatives disclosed in this investigation were synthesized with favorable yields by reacting 1-methyl-3-aminomethylindole with benzotriazole-activated N-protected peptide under microwave heating conditions. The deprotection of the Boc group in compound **5** followed a literature method (Merrifield, 1963) and was achieved by stirring in a mixture of TFA and dichloromethane (1:1) at room temperature for 2 hours. Scheme 1 outlines the synthetic pathways utilized for the preparation of the peptide-indole conjugates.



Scheme 1. Synthetic routs for the indole-peptide conjugates

In the proton spectrum of compound **1**, the amide NH peak is observed as a triplet at 8.18 ppm, while the carbamate NH peak is seen as a doublet at 7.57 ppm. In compound **2**, another mono-peptide-indole conjugate, these NH peaks are observed as a triplet at 8.20 ppm and a doublet at 7.56 ppm, respectively. In compound **1**, the methylene peak of the benzyloxycarbonyl (Z) protecting group resonates as a singlet at 5.02 ppm, while in compound **2**, the *tert*-butyl group of the *tert*-butoxycarbonyl (Boc) protecting group resonates as a singlet at 1.30 ppm. The methylene group at the 3rd position of the indole molecule and the methyl group at the 1st position in compound **1** resonate as a multiplet in the range of 4.55-4.31 ppm and as a singlet at 3.74 ppm, respectively. In compound **2**, the corresponding peaks resonate as a multiplet in the range of 4.55-4.31 ppm and as a singlet at 3.75 ppm. The appearance of multiplets instead of expected doublet peaks for the methylene groups at the 3rd position is attributed to the chiral neighboring group effect. In the carbon-13 spectrum of compounds **1** and **2**, the amide and carbamate carbonyl peaks resonate at 171.4 and 156.5 ppm for compound **1**, and at 171.8 and 155.7 ppm for compound **2**. The remaining proton and carbon peaks align with the suggested structures, as detailed in the accompanying supplementary information. In compounds **3**, **4**, and **5** dipeptide-indole conjugates, the NH peaks appear as follows: 8.26 (t), 8.07 (d), 7.54 (t); 8.28 (t), 8.02 (d), and in the range of 7.46-7.20 ppm along with aromatic protons; and 8.32 (bs), 8.03 (d), in the range of 7.55-6.94 ppm along with aromatic protons.

The NH protons have been confirmed by D₂O exchange. In compounds **3** and **4**, the methylene peaks of the protecting group resonate as a doublet and quartet at 5.03 and 4.99, respectively, instead of

New peptide-indole conjugates and their biological activities

the expected singlet, due to chiral group effects. The methylene group at the 3rd position of the indole molecule and the methyl group at the 1st position appear as a multiplet at 4.42-4.40 ppm and a singlet at 3.78 ppm in compound **3**, as a doublet at 4.41 ppm and a singlet at 3.73 ppm in compound **4**, and as a broad singlet at 4.41 ppm and a singlet at 3.74 ppm in compound **5**. The different splitting of the indole's methylene protons is attributed to chiral effects. In the carbon-13 spectra of compounds **3**, **4**, and **5**, two amide carbonyl peaks and one carbamate carbonyl peak resonate as follows: 172.3, 168.7, and 156.6 ppm; 171.5, 170.8, and 156.4 ppm; and 171.7, 170.8, and 155.6 ppm, respectively. All other proton and carbon peaks are in accordance with the proposed structures. In order to assess the potential effect of the protective group in amino acids on biological activities, the Boc protective group in compound **5** was removed according to literature methods. The most notable information observed in the proton NMR data between compound **5** and compound **6** includes the absence of the *tert*-butoxy group in compound **6**, the emergence of a broad singlet peak at 8.83 ppm attributed to NH₃ with an intensity of 3 units and a slight shift of the aromatic peak group to a lower field.

Differences observed in the carbon-13 spectrum include the disappearance of aliphatic carbon peaks associated with the *tert*-butoxy group along with the carbonyl peak at 155.6 ppm and the appearance of quartet peak groups at 158.4 ppm and 117.6 ppm, attributed to carbon-fluorine couplings from TFA. The differences observed in the carbon-13 spectrum involve the disappearance of aliphatic carbon peaks associated with the *tert*-butoxy group, as well as the carbonyl peak at 155.6 ppm. Additionally, quartet peak groups at 158.4 ppm and 117.6 ppm emerge attributed to carbon-fluorine couplings from trifluoroacetic acid (TFA). The observed changes in the NMR spectra upon the removal of the Boc protective group are consistent with our previous studies.^{15,17}

3.2 Biological Assay

3.2.1 Cytotoxicity Study

As a result of the calculation of the data obtained from readings at 540 nm wavelength in the spectrophotometer, the IC₅₀ (μg/mL) values of each peptide-indole conjugate (**1-6**) against the MCF-7 and A549 cell lines are presented in Table 1 and Figure S26. Microscopic images depicting the effects of peptide-indole conjugates prepared at a concentration of 100 μg/mL on MCF-7 and A549 cell lines are provided in Figures 1 and 2, respectively.

The anticancer activities of the compounds tested against the MCF-7 cell line are observed in Table 1, Figure S26. Upon examination of the table data and figures, it is evident that compound **3**, a dipeptide-indole derivative containing methionine and glycine amino acids, and compound **1**, a mono-peptide-indole derivative containing leucine amino acid, are the most active against the MCF-7 cell line. With the exception of compound **6**, where the protecting group is removed, all compounds demonstrated higher anticancer activity against the MCF-7 cell line compared to cisplatin.

The anticancer activities of the tested compounds against the A549 cell line are observed in Table 1, Figure 1, and Figure 2. Upon examination of the table data and figures, it is evident that compound **4**, a dipeptide-indole derivative containing methionine and phenylalanine amino acids, and compound **1**, a mono-peptide-indole derivative containing leucine amino acid, are the most active against the A549 cell line. With the exception of compound **6**, where the protecting group is removed, all compounds demonstrated higher anticancer activity against the A549 cell line compared to cisplatin.

However, in a general context, the compounds exhibited relatively higher anticancer activity against the MCF-7 cell line than the A549 cell line. When comparing the structures of the compounds with their anticancer activities against MCF-7 and A549 cell lines, there is a lack of parallelism in anticancer activity for compounds other than compound **1**, a mono-peptide-indole derivative containing leucine amino acid, and compound **6**, a dipeptide-indole derivative with the protecting group removed.

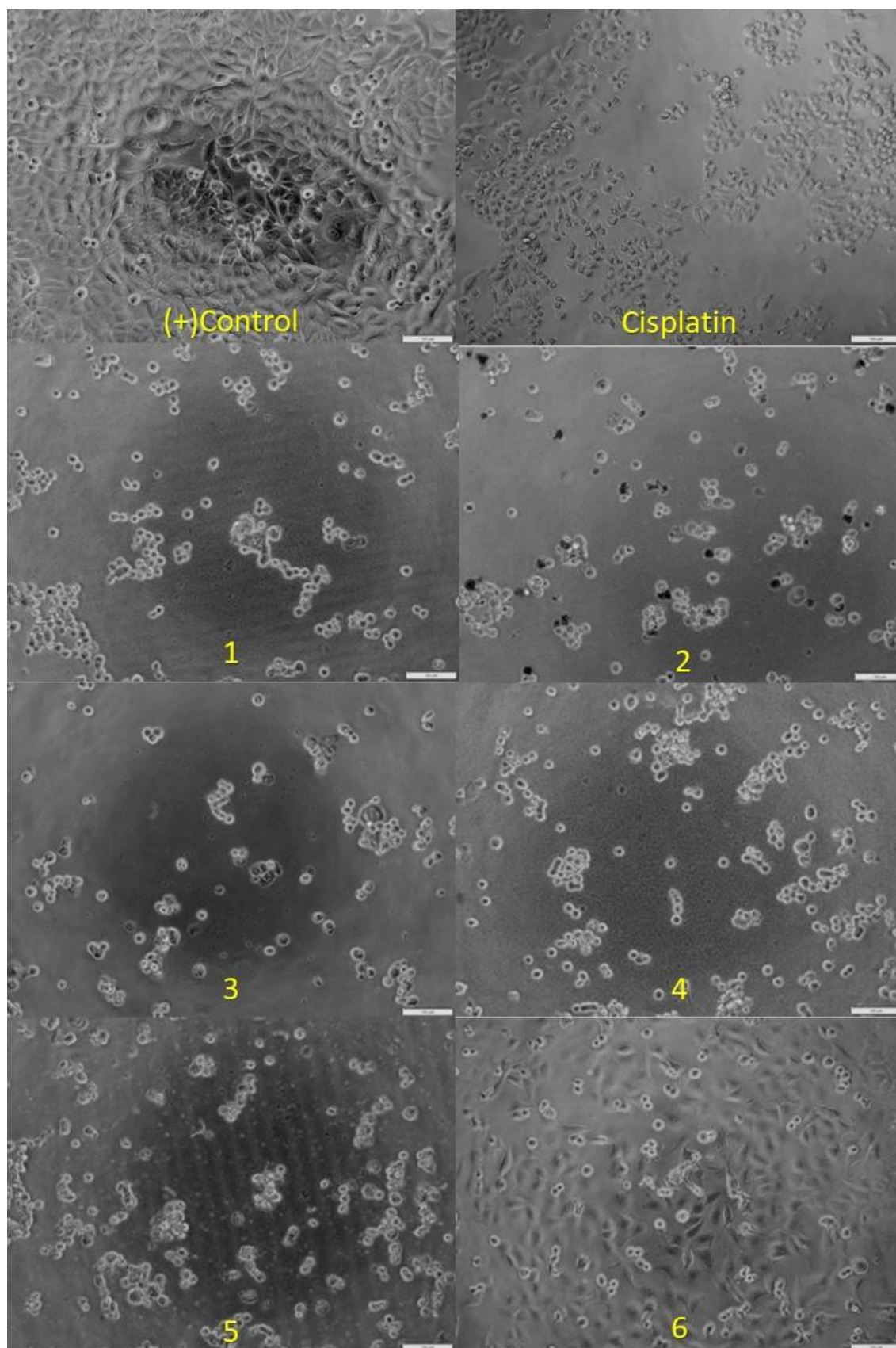


Figure 1. The effect of compounds **1-6** prepared with a concentration of 100 $\mu\text{g/mL}$ on MCF-7 cells

New peptide-indole conjugates and their biological activities

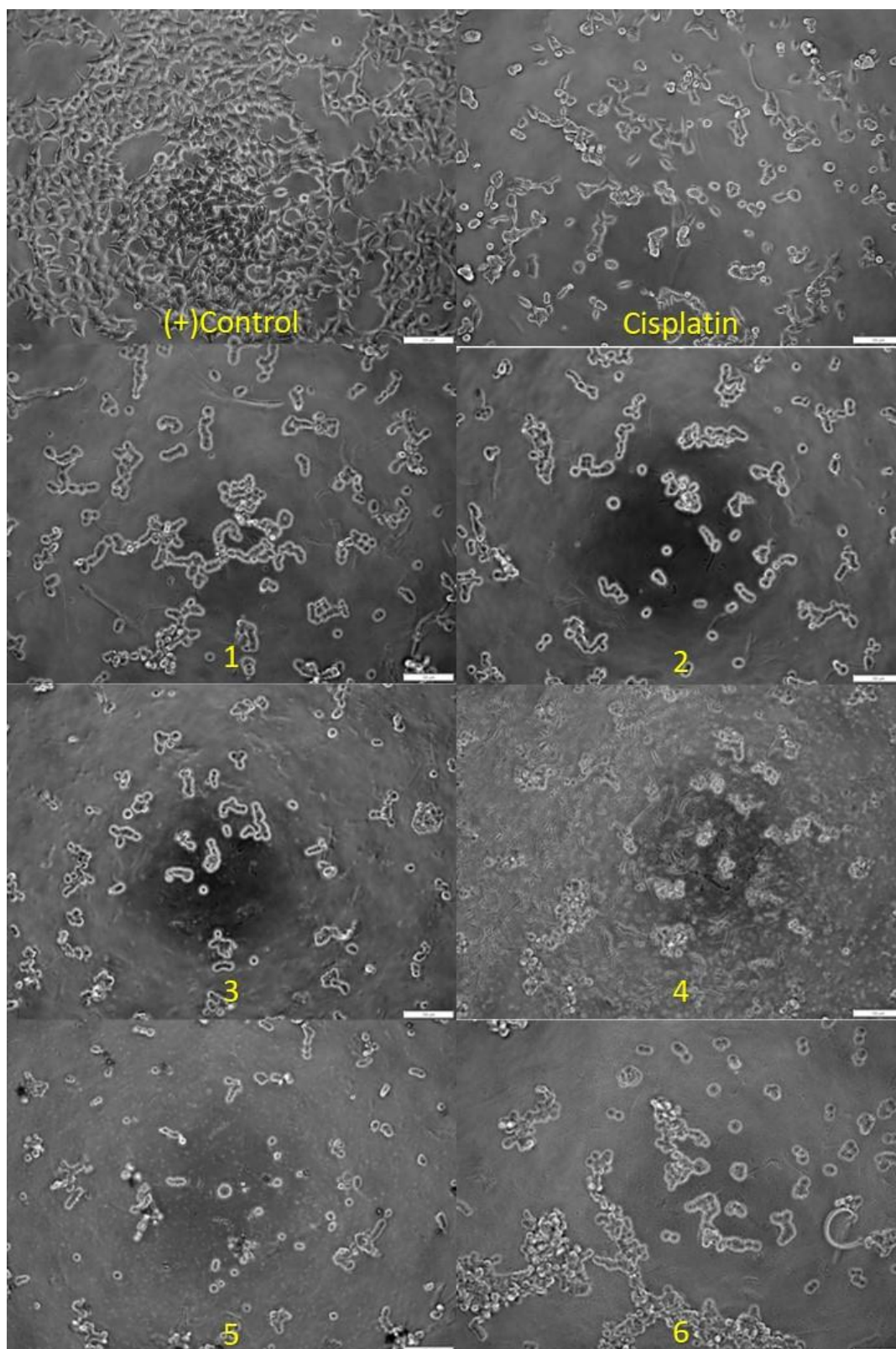


Figure 2. The effect of compounds **1-6** prepared with a concentration of 100 $\mu\text{g/mL}$ on A549 cells. As outlined in the current literature, compounds **1** and **3** among the examined peptide-indole conjugates exhibited antioxidant activities of 26.375% and 22.895%, respectively.

Table 1. IC₅₀ values of compounds **1-6** on MCF-7 and A549 cells

Comp. No	IC ₅₀ (µg/mL)	SD	IC ₅₀ (µg/mL)	
			MCF-7	A549
1	8.72	3.16	3.01	3.01
2	11,36	4,21	2.42	2.42
3	5,86	3,51	3.30	3.30
4	35,03	4,49	1.65	1.65
5	12,12	3,88	2.63	2.63
6	96,86	1,03	4.33	4.33
Cisplatin	82.02	6.19	3.01	3.01

3.2.2. Antioxidant Activity

The assessment of the compounds' antioxidant capacity was conducted through the utilization of the DPPH method²⁰ and the iron reducing potency method,²¹ as outlined in the current literature. Compounds **1** and **3** among the examined peptide-indole conjugates exhibited antioxidant activities of 26.375% and 22.895%, respectively, at a concentration of 125 µg/mL, determined by the DPPH (1,1-diphenyl-2-picrylhydrazyl) method as shown in Table 2.

Table 2. The antioxidant capabilities of the dipeptide-indole conjugates **1-6**

Compound No	DPPH Free Radical Scavenging Activity, %				
	12.5 µg/mL	25 µg/mL	37.5 µg/mL	62.5 µg/mL	125 µg/mL
1	2.126	4.897	8.920	11.123	22.895
2	nd	1.677	3.795	6.714	10.165
3	2.684	5.691	9.026	14.033	26.375
4	3.335	6.691	8.026	10.697	15.369
5	nd	1.045	2.035	5.671	9.342
6	1.238	1.927	2.711	5.724	9.165
BHA	75.167	75.503	76.174	76.845	76.845
BHT	63.758	73.825	75.503	75.838	77.181
α-tocopherol	76.510	77.181	79.530	81.879	84.899

nd: Not detected

Additionally, compounds **3**, **4**, and **5** exhibited the highest antioxidant activities, with values of 0.161%, 0.135%, and 0.121%, respectively, based on the iron reducing power assay as indicated in Table 3. However, in comparison with standard antioxidants such as butylated hydroxyanisole (BHA), butylated hydroxytoluene (BHT), and α-tocopherol, it was generally observed that the indole-peptide conjugates displayed relatively limited antioxidant efficacy in both methods. Furthermore, it was observed that the removal of the protecting group did not enhance the antioxidant activities in either of the methods.

Table 3. The antioxidant capabilities of the dipeptide-indole conjugates **1-6**

Compound No	Iron	Reducing	Activity
	12.5 $\mu\text{g/mL}$	25 $\mu\text{g/mL}$	% 37.5 $\mu\text{g/mL}$
1	0.068	0.091	0.115
2	0.091	0.107	0.113
3	0.095	0.113	0.161
4	0.089	0.098	0.135
5	0.086	0.097	0.121
6	0.084	0.096	0.117
BHA	0,463	1,296	1,927
BHT	0,257	0,491	0,933
α-tocopherol	0.220	0.456	0.778

3.3. Structural Features and Electronic Properties

Theoretical chemistry studies were conducted on the prepared molecules to better understand their molecular geometry and examine their electronic properties. All calculations were performed using the Gaussian 9 package at the B3LYP/6-311G+(d,p) theoretical level. The most stable geometrical structures of molecules **1-6** are illustrated in Figure 3. As seen, none of the structures adopt a linear or planar geometry; instead, they exhibit irregular configurations stabilized by intramolecular hydrogen bonds.

Compounds **1** and **2** feature a single intramolecular hydrogen bond (IHB) between the NH bond of the amide and the CO group of the ester-amide, with distances of 2.13 Å and 2.11 Å, respectively. In contrast, the other molecules exhibit two IHBs with distances ranging from 2.02 to 2.82 Å. These irregular geometries arise from the various substituents present in the dipeptide backbone. On the other hand, the dipole moment of the molecules ranges from 1.56 to 10.13 Debye. The least polarized molecule is **5**, while the most polarized molecule is **6**.

The frontier molecular orbital (FMO) theory, an extension of the molecular orbital (MO) theory, focuses on elucidating the interactions between the most occupied molecular orbital (HOMO) and the least occupied molecular orbital (LUMO) in compounds. The HOMO, positioned like the outer orbital, has electron-donation and nucleophilicity characteristics that determine a compound's reactivity.²⁴ On the other hand, LUMO, which functions like the inner orbital, is electrophilic, i.e. ready to accept electrons. The FMO theory incorporates these orbital characteristics to explain molecular electronic characteristics and reactivity.

The frontier molecular orbital (FMO) theory, an extension of the molecular orbital (MO) theory, focuses on elucidating the interactions between the most occupied molecular orbital (HOMO) and the least occupied molecular orbital (LUMO) in compounds. The HOMO, positioned like the outer orbital, has electron-donation and nucleophilicity characteristics that determine a compound's reactivity. On the other hand, LUMO, which functions like the inner orbital, is electrophilic, i.e. ready to accept electrons. The FMO theory incorporates these orbital characteristics to explain molecular electronic characteristics and reactivity.

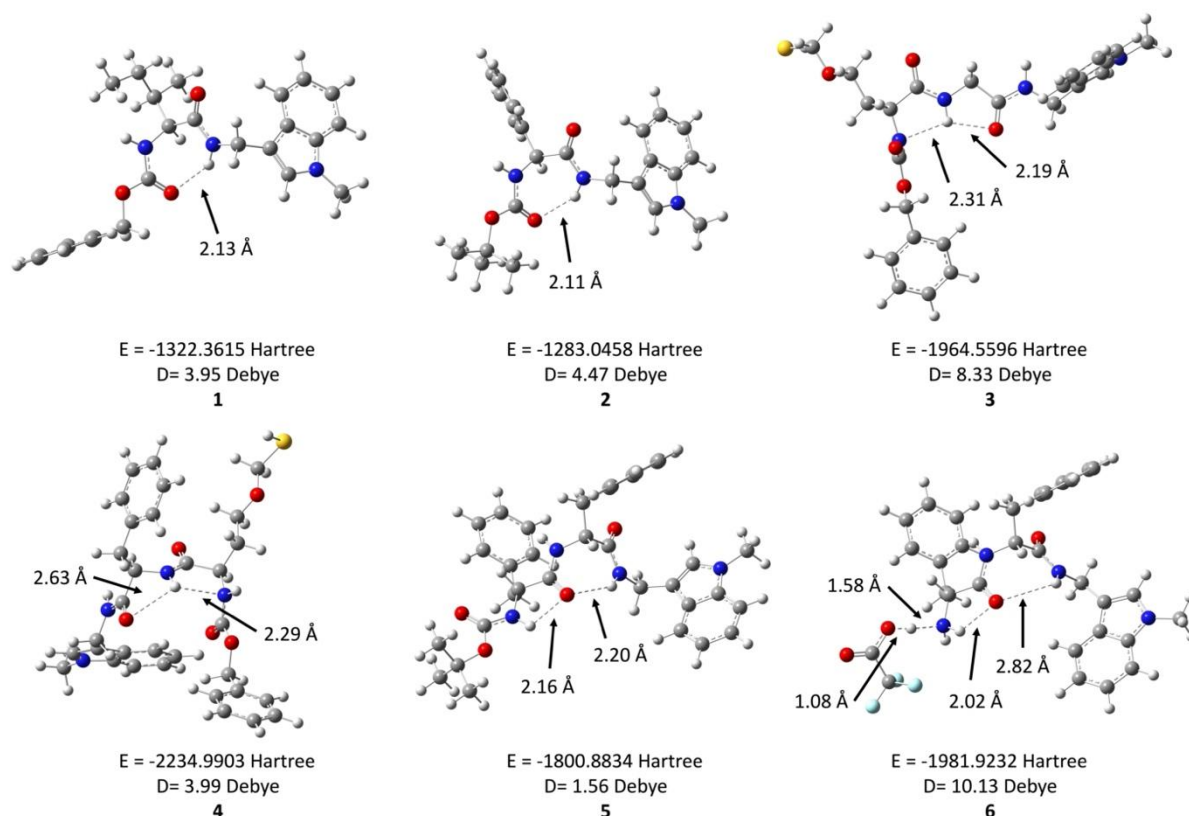


Figure 3. Optimized molecular geometry of molecules **1-6** at the B3LYP/6-311G+(d,p) level

The distribution of FMOs for molecules **1-6** is shown in Figure 4. It is clear that the HOMO of all the molecules share a similar pattern, mainly located on the indole ring. This observation implies that the indole serves as the determining site for the reactivity of this type of molecule towards electrophiles. On the other hand, the LUMOs exhibit variations across the molecules. In molecule **1**, the LUMO is located on the benzyl group, while in molecule **2**, which shares a similar geometry to **1**, the LUMO is distributed throughout the molecule. In the case of molecules **3** and **4**, the LUMO is distributed exclusively on the indole and benzyl groups, respectively. For molecules **5** and **6**, the HOMO is located on one of the benzyl groups positioned between the amide and ester-amide groups. These results indicate that the LUMOs of these compounds, representing the electrophilic sites, depend on the nature of the substituents.

The FMO theory focuses on another critical parameter known as the HOMO-LUMO energy gap (ΔE). This energy difference has key implications for the chemical characteristics of a molecule. A high ΔE means greater thermodynamic stability, indicating the robustness of the compound.²⁵ Conversely, a lower ΔE suggests a propensity for easy electronic transitions, implying a more dynamic and potentially reactive molecular state. The correlation between HOMO energy (E_{HOMO}) and ionization potential, and the association between LUMO energy (E_{LUMO}) and electronic affinity, contribute to a better understanding of molecular behaviour.²⁶ E_{HOMO} elucidates the molecule's tendency to lose an electron, while E_{LUMO} highlights its affinity to gain an electron. The FMO and ΔE energies of the studied compounds are shown in Figure 4. The E_{HOMO} s range from -5.54 to -6.03 eV, suggesting that compound **2**, with the highest value, is the most electron donor, while compound **3**, with the lowest value, is the least electron donor. The E_{LUMO} values range from -0.64 to -1.08 eV. Compound **2**, with the highest value, has the lowest electron acceptance capacity, while compound **6**, with the lowest value, has the highest electron acceptance capacity. Furthermore, the ΔE trend is **1** < **5** = **6** < **4** < **2** < **3**, indicating that compound **1** is the most chemically reactive, while compound **3** is the most chemically stable.

New peptide-indole conjugates and their biological activities

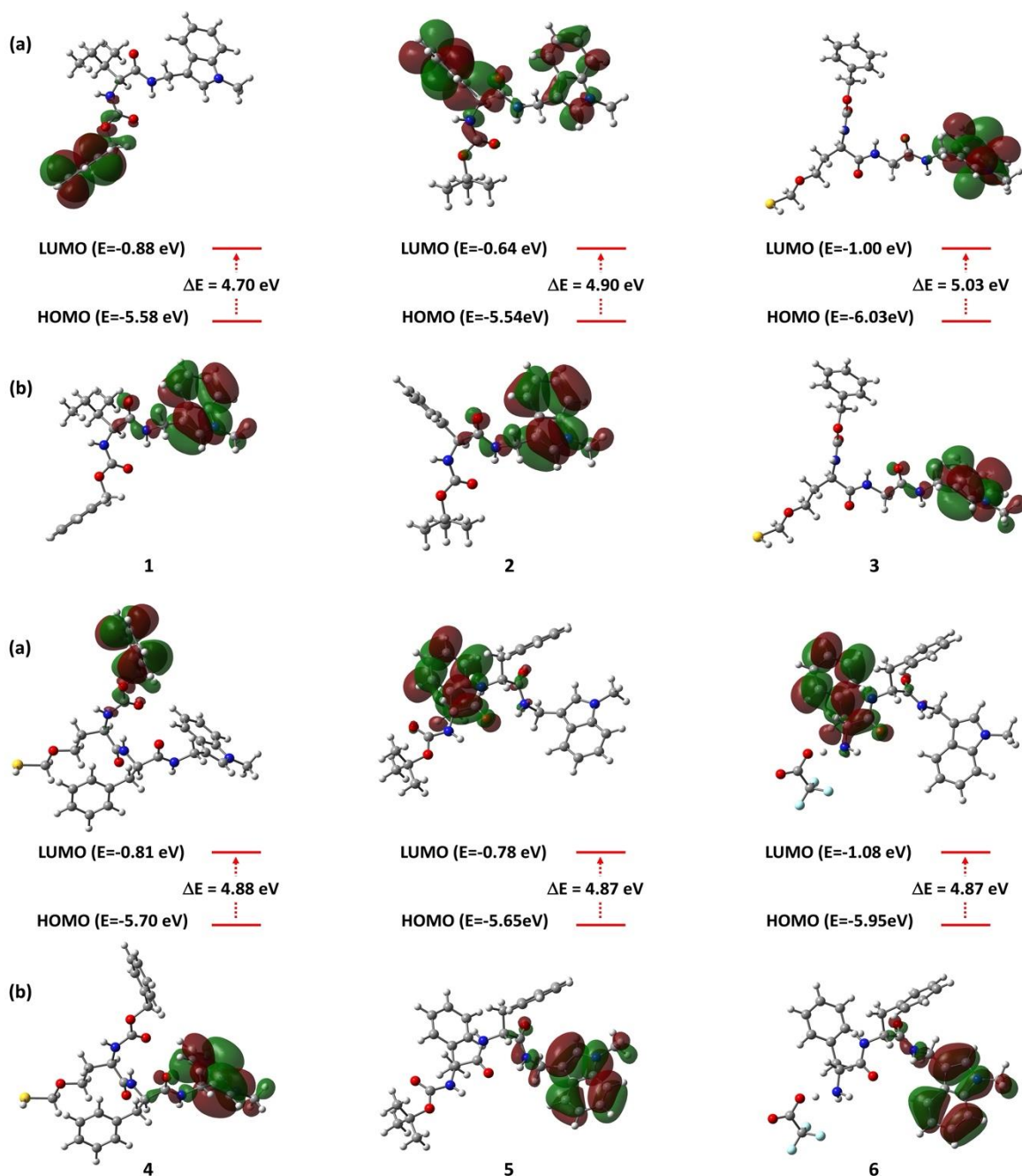


Figure 4. Distribution and energies of FMOs of compounds **1-6** calculated at the B3LYP/6-311G+(d,p) level

The electrostatic potential (ESP) is an essential parameter that gives crucial information about the reactivity of molecules, in particular about potential interaction sites with biological molecules such as DNA and enzymes. Figure 5 depicts the ESPs of the molecules studied, using color-coding to indicate electron-rich and electron-poor regions. Electron-rich regions are shown in red, while electron-poor regions are shown in blue. Examination of the figure reveals multiple electron-rich sites in all the molecules, mainly associated with carbonyl groups. This observation implies that these specific sites are ready to engage in interactions with biological molecules, potentially forming hydrogen bonds and assuming the role of acceptors. On the other hand, all molecules also present electron-poor sites that could actively participate in hydrogen bonding as donors, mainly located on NH groups.

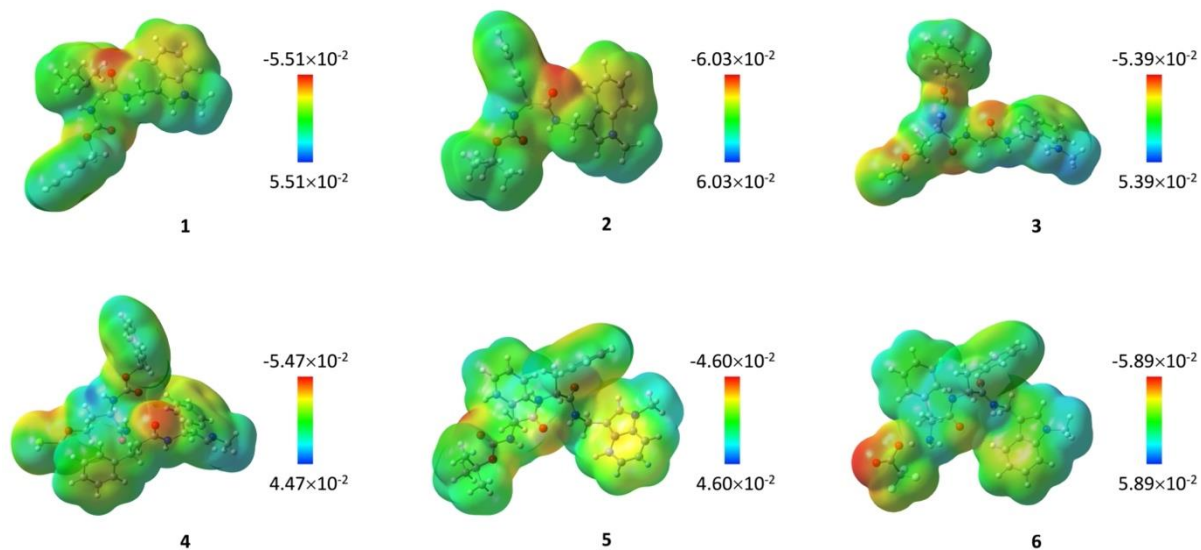


Figure 5. Electrostatic potential maps of compounds **1-6** calculated at the B3LYP/6-311G+(d,p) level

3.3.1. Molecular Docking Studies

Molecular docking studies including binding modes/orientations, affinities, and interaction analysis were performed on the most active compounds (**1-5**) against the EGFR (epidermal growth factor receptor, PDB code: 2ITY) target. EGFR is a cell surface receptor that plays a crucial role in regulating cell growth and survival. It belongs to the ErbB family of receptors and, when activated by binding to its ligands, such as epidermal growth factor (EGF), triggers a series of signaling pathways that contribute to cell proliferation, differentiation and survival.

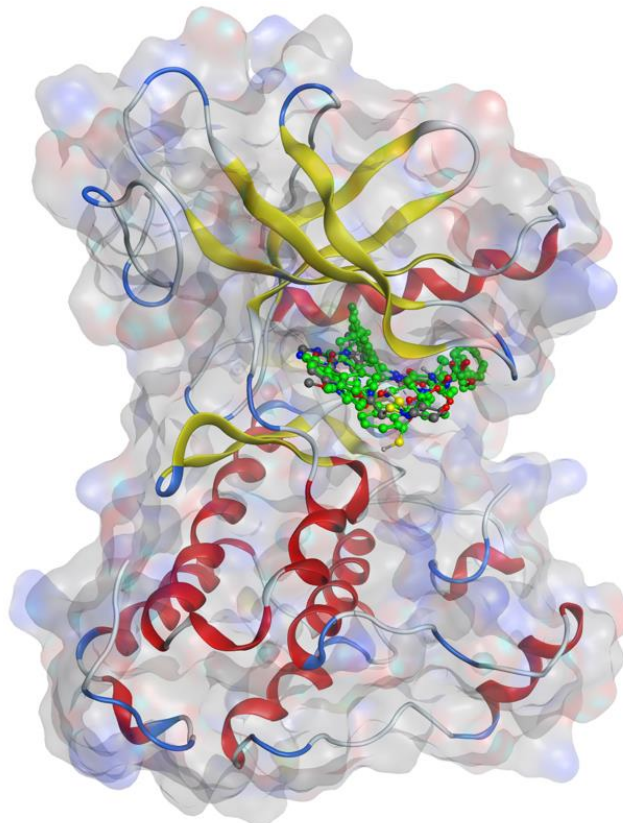


Figure 6. Orientation of the most stable docking pose of compounds **1-5** and Gefitinib into EGFR

New peptide-indole conjugates and their biological activities

In the context of cancer, dysregulation of EGFR signaling is often associated with the development and progression of various types of cancer. EGFR mutations or overexpression can lead to uncontrolled cell growth and tumor formation. Targeting EGFR has therefore become an important strategy in the development of cancer therapies.^{27,28} In this context, EGFR has been reported to be the target of several indole-based anticancer molecules.²⁹⁻³¹

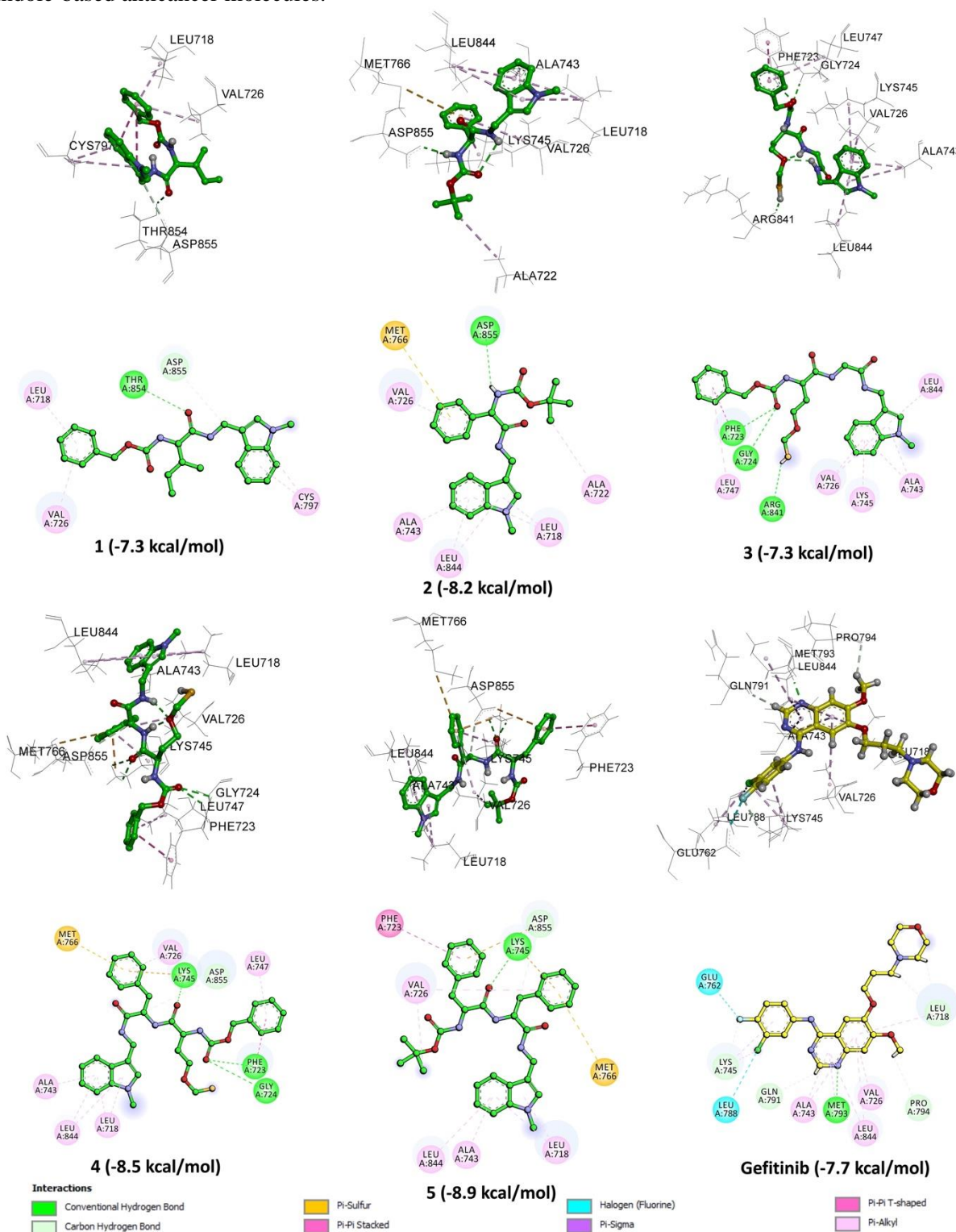


Figure 7. Binding modes and energies of compounds **1-5** and Gefitinib into EGFR

The obtained results of the docking study indicate that the most energetically stable orientation for all compounds is situated in the same region as the Gefitinib inhibitor within the active site of the enzyme (Figure 6). The binding energies fall within the range of -7.3 to -8.9 kcal/mol, comparable to or lower than that of Gefitinib (-7.7 kcal/mol), suggesting a high affinity of all tested molecules for this enzyme. The interaction analysis, as depicted in Figure 7, reveals that compounds **1** and **2** form a hydrogen bond with THR854 and ASP855 via the carbonyl and NH groups, respectively. Compound **3** establishes three hydrogen bonds with PHE723, GLY724, and ARG841 through the carbonyl and SH groups. Similarly, compound **4** is engaged in three hydrogen bonds with LYS745, PHE723, and GLY724 via two carbonyl moieties. On the other hand, compound **5** forms a hydrogen bond with LYS745 through the carbonyl group. In comparison, Gefitinib forms a single hydrogen bond with MET793. Furthermore, all the molecules exhibit favorable hydrophobic, halogenic, and other weak binding interactions with various amino acids within the active site. These findings suggest that all the molecules possess a strong affinity for EGFR by interacting with critical amino acids in the active site, indicating their potential as inhibitors of this enzyme. Additionally, these results underscore the significance of the carbonyl groups of the molecule in the interaction with EGFR.

4. Conclusion

Breast cancer is a highly prevalent type of cancer and is the most commonly occurring cancer in women. On the other hand, lung cancer is the second most frequent cancer and the primary cause of cancer-related deaths. The prolonged use of current anticancer drugs is associated with severe side effects and a high mortality rate. Generally, there is an inverse correlation between compounds with antioxidant activity and cancer. For these reasons, studies focusing on the synthesis of new compounds with low side effects, efficacy, and yet to be resistant to cancer cell lines, along with screenings for their anticancer and antioxidant properties, are crucial. In the scope of this study, new peptide-indole derivatives were synthesized, and their anticancer activities against MCF-7 and A549 cell lines, as well as their antioxidant capacities using DPPH and iron reduction power methods, were determined. Among the investigated compounds, it was found that the monopeptide-indole derivative containing leucine amino acid and the dipeptide-indole derivatives containing methionine exhibited higher anticancer activity.

Generally, compounds, except compound **6** where the protecting group is removed, showed higher activity compared to cisplatin. However, the antioxidant activities of the compounds were lower compared to the standard antioxidants used.

Acknowledgements

We express our gratitude to İnönü University, Turkey, for providing financial support through BAPB Grand No-FOA-2020-2203.

Supporting Information

Supporting information accompanies this paper on <http://www.acgpubs.org/journal/organic-communications>

ORCID

Hasan Küçükbay: [0000-0002-7180-9486](https://orcid.org/0000-0002-7180-9486)

Zeynep Gönül: [0000-0003-4871-4267](https://orcid.org/0000-0003-4871-4267)

Ali Kuruçay: [0000-0002-8816-0425](https://orcid.org/0000-0002-8816-0425)

Burhan Ateş: [0000-0001-6080-229X](https://orcid.org/0000-0001-6080-229X)

Houssein Boulebd: [0000-0002-7727-8583](https://orcid.org/0000-0002-7727-8583)

F. Zehra Küçükbay: [0000-0001-7784-4138](https://orcid.org/0000-0001-7784-4138)

References

- [1] Dorababu, A. Indole – a promising pharmacophore in recent antiviral drug discovery. *RSC Med. Chem.* **2020**, *11*, 1335–1353.
- [2] Kumar, S. A. Brief review of the biological potential of indole derivatives. *Futur. J. Pharm. Sci.* **2020**, *6*:121, 1–19.
- [3] Sravanthi, T. V.; Manju, S. L. Indoles - a promising scaffold for drug development. *Eur. J. Pharm. Sci.* **2016**, *91*, 1–10.
- [4] Zhang, X.; Cui, Y.; Katoh, R.; Koumura, N.; Hara, K. Organic dyes containing thieno [3 , 2- b] indole donor for efficient dye-sensitized solar cells. *J. Phys. Chem. C.* **2010**, *114*, 18283–18290.
- [5] Qian, X.; Yan, R.; Hang, Y.; Lv, Y.; Zheng, L.; Xu, C.; Hou, L. Dyes and pigments indeno [1 , 2- b] indole-based organic dyes with different acceptor groups for dye-sensitized solar cells. *Dye Pigment.* **2017**, *139*, 274–282.
- [6] Dai, P.; Zhu, Y.; Liu, Q.; Yan, Y.; Zheng, J. Novel indeno [1 , 2- b] indole-spirofluorene donor block for efficient sensitizers in dye-sensitized solar cells. *Dyes Pigment.* **2020**, *175*, 108099.
- [7] Matsui, M.; Ito, A.; Kotani, M.; Kubota, Y.; Funabiki, K.; Jin, J.; Yoshida, T.; Minoura, H.; Miura, H. The Use of indoline dyes in a zinc oxide dye-sensitized solar cell. *Dyes Pigment.* **2009**, *80* (2), 233–238.
- [8] Bandini, M.; Eichholzer, A. Catalytic Functionalization of indoles in a new dimension. *Angew. Chemie - Int. Ed.* **2009**, *48* (51), 9608–9644.
- [9] Sepehri, S.; Heiran, R.; Ghasemi, Y.; Turos, E. Molecular docking, synthesis and evaluation of the antimicrobial, antiproliferative, and antioxidant properties of β -lactam bisindoles. *J. Mol. Struct.* **2023**, 136298.
- [10] Wang, X.; Su, H.; Chen, C.; Cao, X. Synthesis and biological evaluation of peptidomimetics containing the tryptamine moiety as a potential antitumor agent. *RSC Adv.* **2015**, *5* (20), 15597–15602.
- [11] Weng, J.; Tsai, C.; Kulp, S. K.; Chen, C. Indole-3-carbinol as a chemopreventive and anti-cancer agent. *Cancer Lett.* **2008**, *262*, 153–163.
- [12] Higdon, J. V.; Delage, B.; Williams, D. E.; Dashwood, R. H. cruciferous vegetables and human cancer risk: epidemiologic evidence and mechanistic basis. *Pharmacol. Res.* **2007**, *55* (3), 224–236.
- [13] Yan, X.-Jie; Qi, M.; Telusma, G.; Yancopoulos, S.; Madaio, M.; Satoh, M.; Reeves, W. H.; Teichberg, S.; Kohn, N.; Auborn, K.; Chiorazzi, N. Indole-3-carbinol improves survival in lupus-prone mice by inducing tandem b- and t-cell differentiation blockades. *Clin. Immunol.* **2009**, *131* (3), 481–494.
- [14] Li, Z.; Ding, B.; Ali, M. R. K.; Zhao, L.; Zang, X.; Lv, Z. Dual effect of tryptamine on prostate cancer cell growth regulation: a pilot study. *Int. J. Mol. Sci.* **2022**, *23* (19), 11087.
- [15] Gönül, Z.; Öztürk, D. A.; Küçükbay, F. Z.; Tekin, S.; Tekin, Z.; Küçükbay, H. Antioxidant and cytotoxic properties of some new dipeptide-indole conjugates. *J. Heterocycl. Chem.* **2023**, *60*, 86-95.
- [16] El Khatib, M.; Jauregui, L.; Tala, S. R.; Khelashvili, L.; Katritzky, A. R. Solution-phase synthesis of chiral o-acyl isodipeptides. *Medchemcomm* **2011**, *2* (11), 1087.
- [17] Küçükbay, H.; Parladi, F. M.; Küçükbay, F. Z.; Angeli, A.; Bartolucci, G.; Supuran, C. T. Synthesis, Antioxidant and carbonic anhydrase inhibitory properties of mono-peptide-anthraquinone conjugates. *Org. Commun.* **2021**, *14* (3), 255–269.
- [18] Buğday, N.; Küçükbay, F. Z.; Küçükbay, H.; Bua, S.; Bartolucci, G.; Leitans, J.; Kazaks, A.; Tars, K.; Supuran, C. T. Synthesis of Novel dipeptide sulfonamide conjugates with effective carbonic anhydrase I, II, IX, and XII Inhibitory properties. *Bioorg. Chem.* **2018**, *81*, 311–318.
- [19] Denizot, F.; Lung, R. Unifying an investment portfolio within a donor advised fund. *J. Immunol. Methods* **1986**, *89*, 271–278.
- [20] Yang, J.; Guo, J.; Yuan, J. In vitro antioxidant properties of rutin. *LWT - Food Sci. Technol.* **2008**, *41* (6), 1060–1066.
- [21] Oyaizu, M. Studies on products of browning reaction. antioxidative activities of products of browning reaction prepared from glucosamine. *Japanese J. Nutr. Diet.* **1986**, *44* (6), 307–315.
- [22] Frisch, M. J.; Trucks, G. W.; Schlegel, H. B.; Scuseria, G. E.; Robb, M. A.; Cheeseman, J. R.; Scalmani, G.; Barone, V.; Mennucci, B.; Petersson, G. A.; Nakatsuji, H.; Caricato, M.; Li, X.; Hratchian, H. P.; Izmaylov, A. F.; Bloino, J.; Zheng, G.; Sonnenberg, J. L.; Hada, M.; Ehara, M.; Toyota, K.; Fukuda, R.; Hasegawa, J.; Ishida, M.; Nakajima, T.; Honda, Y.; Kitao, O.; Nakai, H.; Vreven, T.; Montgomery, J. A.; Peralta, J. E.; Ogliaro, F.; Bearpark, M.; Heyd, J. J.; Brothers, E.; Kudin, K. N.; Staroverov, V. N.; Kobayashi, R.; Normand, J.; Raghavachari, K.; Rendell, A.; Burant, J. C.; Iyengar, S. S.; Tomasi, J.; Cossi, M.; Rega, N.; Millam, J. M.; Klene, M.; Knox, J. E.; Cross, J. B.; Bakken, V.; Adamo, C.; Jaramillo, J.; Gomperts, R.; Stratmann, R. E.; Yazyev, O.; Austin, A. J.; Cammi, R.; Pomelli, C.; Ochterski, J. W.; Martin, R. L.; Morokuma, K.; Zakrzewski, V. G.; Voth, G. A.; Salvador, P.; Dannenberg, J. J.; Dapprich, S.; Daniels, A.

- D.; Farkas; Foresman, J. B.; Ortiz, J. V.; Cioslowski, J.; Fox, D. J. Gaussian 09, Revision B.01. *Gaussian 09, Revis. B.01, Gaussian, Inc., Wallingford CT.* **2009**, 1–20.
- [23] Trott, O.; Olson, A. J.; AutoDock Vina: improving the speed and accuracy of docking with a new scoring function, efficient optimization, and multithreading. *J. Comput. Chem.* **2010**, *31* (2), 455–461.
- [24] Boulebd, H. Insights on the antiradical capacity and mechanism of phytocannabinoids: h-abstraction and electron transfer processes in physiological media and the influence of the acid-base equilibrium. *Phytochemistry* **2023**, *208*, 113608.
- [25] Lewis, D. F. V.; Ioannides, C.; Parke, D. V.; Interaction of a series of nitriles with the alcohol-inducible isoform of P450: computer analysis of structure - activity relationships. *Xenobiotica* **1994**, *24* (5), 401–408.
- [26] Boulebd, H. Structure-activity relationship of antioxidant prenylated (iso)flavonoid-type compounds: quantum chemistry and molecular docking studies. *J. Biomol. Struct. Dyn.* **2022**, *40* (20), 10373–10382.
- [27] Pallis, A. G.; Serfass, L.; Dziadziusko, R.; van Meerbeeck, J. P.; Fennell, D.; Lacombe, D.; Welch, J.; Gridelli, C. Targeted therapies in the treatment of advanced/metastatic nscl. *Eur. J. Cancer* **2009**, *45* (14), 2473–2487.
- [28] Ramalingam, S. S.; Owonikoko, T. K.; Khuri, F. R. Lung cancer: new biological insights and recent therapeutic advances. *CA. Cancer J. Clin.* **2011**, *61* (2), 91–112.
- [29] Oberhuber, N.; Ghosh, H.; Nitzsche, B.; Dandawate, P.; Höpfner, M.; Schobert, R.; Biersack, B. synthesis and anticancer evaluation of new indole-based tyrphostin derivatives and their (*p*-cymene)dichloridoruthenium(II) complexes. *Int. J. Mol. Sci.* **2023**, *24* (1), 854.
- [30] Zhang, G.; Tang, Z.; Fan, S.; Li, C.; Li, Y.; Liu, W.; Long, X.; Zhang, W.; Zhang, Y.; Li, Z.; Wang, Z.; Chen, D.; Ouyang, G. synthesis and biological assessment of indole derivatives containing penta-heterocycles scaffold as novel anticancer agents towards A549 and K562 cells. *J. Enzyme Inhib. Med. Chem.* **2023**, *38* (1), 2163393.
- [31] Perike, N.; Edigi, P. K.; Nirmala, G.; Thumma, V.; Bujji, S.; Naikal, P. S. Synthesis, anticancer activity and molecular docking studies of hybrid molecules containing indole-thiazolidinedione-triazole moieties. *ChemistrySelect* **2022**, *7* (e20220377), 1–10.

A C G
publications

© 2024 ACG Publications